Simulation of a Slab of Random Particulate Medium Containing Metal Clusters

Sumitomo Chemical Co., Ltd.
IT-Related Chemicals Research Laboratory
Saswatee BANERJEE
Kiyoharu NAKATSUKA

We discuss a simulation method to compute the collimated or the angle-dependent diffuse reflection and transmission of a dielectric slab containing randomly distributed dielectric or metal inclusions. The illumination can either be coherent, incoherent or partially coherent. We solve a multiflux formulation of scalar radiative transfer equation (SRTE) for the purpose. The scattering and extinction cross-sections and the phase function of a single spherical inclusion are computed using Mie analytical theory. In the case of non-spherical scattering centres, we compute the scattering characteristics using a three dimensional finite-difference time-domain (FDTD) method and a near-to-far field transformation integral. For metal inclusions, a recursive convolution FDTD that implements a 1st order Drude model is used. The near-to-far field transformation is achieved by numerically implementing the well-known Rayleigh-Sommerfield integral for the propagation of the scalar field components. The simulation method can be used to investigate various nano-structured devices made from composite media for novel optical properties.

This paper is translated fr om R&D Repor t, “SUMITOMO KAGAKU”, vol. 2010- I.

Introduction

A computer color matching (CCM) or computerized colorant formulation system based on the 2-flux theor y have been developed in this company[1]. These computation modules became central to the quality management process of pigments and dyes while stimulating development in pigment and dye based applications. Now-a-days this technology is employed in the pr oduction of the color filters used in liquid crystal displays (LCD) and the pigment resist needed to fabricate the color filters. However, computation techniques more sophisticated than the 2 flux theor y are needed to compute the optical characteristics of the moder n high performance diffusers, the anti-glare films and the high color saturation, high contrast color filters. For example, when the colorants are added in high concentrations, the coherent interactions between light scattered from constituent particles in particle aggregates have to be taken into consideration. Also, when pigments are dispersed in a medium containing high concentration of dye, the absorption due to the medium (effect of the imaginary part of the r efractive index) can not be neglected. Furthermore, it has become necessary to analyze the colorants that utilize the plasmon resonances of metal nano particles. Here, we outline a simulation scheme that combines various numerical techniques, such as, Monte Carlo, finite-difference time-domain method (FDTD) and multi-flux radiative transfer method to compute the optical characteristics of slabs of complex media as described above.

One can solve the scalar radiative transfer equation (SRTE) to compute the reflection and transmission spectra of a slab of random par ticulate medium under coherent, incoherent or partially coherent illumination[2]. We implemented an N-flux version of SR TE for this purpose[3, 4]. Each of the N fluxes represents collimated or diffuse flux propagation in various angular channels. Each angular channel is an annulus of solid angle, specified by a unique polar angle, a given width and spans over 2π azimuth angles (ϕ). The SRTE is formulated in ter ms of the physically measurable properties such as, the extinction and scattering cross-sections or the phase function of the single inclusion that serves as the smallest scattering centre. The extinction and scattering cross-sections or the phase function of a single spherical scattering centre can be computed analytically using the Mie theory[5]. However, inclusions are not always spheres, and as the concentration of inclusions increases the coherent

interaction among particles becomes important. Even at low concentration, homogeneous dispersion of inclusions throughout the binder medium cannot be ensured. If clusters of inclusions for m, the smallest scattering centres may not be spherical. T o study the effect of non-spherical scattering centres we propose a novel computational method.

In case of inclusions with arbitrar y shapes and sizes we use three-dimensional finite-difference time-domain (FDTD) algorithm that is developed in-house. The FDTD computes the scattered fields of an inclusion at a near field point. The far-field scattering characteristics can be computed using a near-to-far field transformation integral. In case of inclusions made of noble metals a recursive convolution FDTD (RC-FDTD) is used [6), 7)]. The RC-FDTD implements the 1st order Drude model to account for the wavelength dependence of the metal dielectric constant.

To compute the r eflection or transmission characteristics of a slab that contains clusters of inclusions, we first generate a random cluster of inclusions[8)]. We use a random number generator algorithm to generate a random configuration of inclusions. We compute the extinction and scattering cr oss-sections or the phase function for this computationally generated cluster using the FDTD and the near-to-far field transformation integral. The scattering characteristics are averaged over many clusters each containing different random configuration of inclusions. Finally, the average values of scattering characteristics are used in the SRTE formulation to determine the reflection or transmission spectra of the slab. This computational scheme actually suggests a way to incorporate FDTD r esults into an N-flux formulation of SRTE.

Since our actual computation method is a combination of different numerical methods, we include brief introduction of each constituent method. The paper is organized in the following way , in Section 2, we briefly introduce the N-flux formulation and solution technique for the scalar radiative transfer equation (SRTE). Section 3 discusses a brief introduction to the in-house RC-FDTD algorithm implementing 1st order Drude model. The corresponding FDTD update equations for the non-dispersive or dielectric case are also pointed out. The overall computation scheme to incorporate FDTD results in SRTE formulations will be described in Section 4. Section 5 details the r esults of numerical experiments with the simulation method proposed in this paper. Finally, we discuss the conclusions in Section 6.

N-Flux Scalar Radiative Transfer Equation

1. Formulation

The SRTE is a mathematical representation of energy conser vation principle. It deals with the transpor t of a scalar quantity called 'flux', which is a measur e of energy associated with the incident or scattered light, through the random medium.

To formulate the energy transport equation associated with propagation of radiation through a discrete random medium, let us consider a cylindrical volume element, length of which is $d\tau$ and the cross-sectional area is dA. τ is known as the optical depth or optical thickness and is the product of the physical thickness or distance (x) and the number of scattering centres per unit volume of the medium. The light that is pr opagating in this volume element can be either coherent or incoherent. Coher ent and incoher ent fluxes ar e associated with the collimated and dif fuse par ts of incident light respectively. The reason for separating these two fluxes is physical. Collimated and dif fuse fluxes behave differently. The collimated flux can only be lost from the volume element while diffused flux can both be lost and gained. Two physical mechanisms are responsible for this flux loss and gain: one is absorption, other is scattering. These two effects are accounted for by scattering and absorption cross-sections of the inclusions respectively, assuming that the host matrix is both absorption-free and scattering-free. Also, for the diffuse flux the gain can be due to the scattering of the collimated flux within the same volume element or the scattering of the diffuse flux in neighboring volume elements.

Let us denote the forward moving ($+x$) collimated flux by f_{c+}, the backward moving ($-x$) collimated flux by f_{c-}, the forward moving ($+x$) diffuse flux by f_{d+}, the backward moving ($-x$) diffuse flux by f_{d-}. However, in case of diffuse flux, to account for directional propagation we assign a symbol f_{d+}^{i} to represent the forward moving flux in the ith direction. In our case the ith direction is called the ith channel, defined by an annulus of solid angle $\delta\omega_i$, specified by a polar angle θ_i, a width $\delta\theta_i$ and spanning over the entire range of the azimuth angles (ϕ) from 0 to 2π. Thus, we defined N–1 channels for the propagation of the diffuse flux. The channel indices 1 to $N/2$–1 are associated with the for ward moving dif fuse fluxes. The rest of the channels are for the backward moving diffuse flux. 0th and Nth channels are reserved for the collimated flux propagating in the forward and

backward directions respectively. Using our notations a column vector F, can be defined, the elements of which represent the collimated and the diffuse fluxes in different channels as follows

$$F = \begin{bmatrix} f_{c+} \\ f_{d+}^{1} \\ \vdots \\ f_{d+}^{N/2-1} \\ f_{d-}^{N/2} \\ \vdots \\ f_{d-}^{N-1} \\ f_{c-} \end{bmatrix} \qquad \text{(Eq. 1)}$$

Taking the loss of collimated flux due to scattering and absorption into consideration, we can write the flux balance equation for channel 0 as follows:

$$\frac{df_{c+}}{dx} = -kf_{c+} - S_1 f_{c+} - S_2 f_{c+} \qquad \text{(Eq. 2)}$$

where $\frac{df_{c+}}{dx}$ represents the rate of change of forward moving collimated flux per unit length. The first term on the right hand side of Eq. (2) accounts for the loss of flux from the channel by absorption. The last two terms represent the total loss of flux from the channel by scattering. The first scattering coefficient S_1 accounts for the flux loss fr om channel 0 to all the for ward moving diffuse channels identified by indices 1 to $N/2$–1. The second scattering coefficient S_2 accounts for the flux loss from the channel to all the backward moving diffuse channels identified by indices $N/2$ to N–1. k, S_1 and S_2 can be computed in terms of the absorption and scattering characteristics of a single particle. Explicit expressions for k, S_1 and S_2 are given in Section 2.3.

The flux balance equation for Nth channel (for ward moving collimated flux) as follows:

$$-\frac{df_{c-}}{dx} = -kf_{c-} - S_1 f_{c-} - S_2 f_{c-} \qquad \text{(Eq. 3)}$$

where the extra '-' sign on the left hand side of Eq. (3) accounts for the backwar d propagation of the flux. Other symbols have the same physical meaning as in Eq. (2).

The flux balance equation for the ith forward moving diffuse channel is given by

$$\frac{df_{d+}^{i}}{dx} = -\frac{Kf_{d+}^{i}}{|\cos\theta_i|} - \frac{1}{4\pi}\frac{f_{d+}^{i}}{|\cos\theta_i|}\int_{j\neq i} p(\hat{\mathbf{n}}_j, \hat{\mathbf{n}}_i)\, d\omega_j + \frac{1}{4\pi}\int_{j\neq i}\frac{f_{d\pm}^{j}}{|\cos\theta_j|} p(\hat{\mathbf{n}}_i, \hat{\mathbf{n}}_j)\, d\omega_j + S1_i f_{c+} + S2_i f_{c-} \qquad \text{(Eq. 4)}$$

The first term on the right hand side of Eq. (4) accounts for the loss of flux due to absorption. The second term on the right hand side of Eq. (4) is associated with the loss of flux due to scattering of light out of the ith channel to all the other diffuse channels. $p(\hat{\mathbf{n}}_j, \hat{\mathbf{n}}_i)$ is the phase function, that gives the scattered intensity in channel j when the scattering centr e is in channel i. $\hat{\mathbf{n}}_i$ and $\hat{\mathbf{n}}_j$ are two unit vectors along i and j directions respectively. The third term on the right hand side of Eq. (4) gives the flux gain in the ith channel due to the scattered light coming from all the other j channels. $p(\hat{\mathbf{n}}_i, \hat{\mathbf{n}}_j)$ is the phase function giving the amount of light that is scattered in channel i when the light is incident on a scattering centre in channel j. $\hat{\mathbf{n}}_i$ and $\hat{\mathbf{n}}_j$ are two unit vectors along i and j directions respectively. The fourth and fifth terms on the right hand side of Eq. (4) give the flux gain due to scattering of forward and backward moving collimated fluxes respectively.

A flux balance equation similar to Eq. (4) for the backward-moving diffuse flux (f_{d-}) is given by

$$-\frac{df_{d-}^{i}}{dx} = -\frac{Kf_{d-}^{i}}{|\cos\theta_i|} - \frac{1}{4\pi}\frac{f_{d-}^{i}}{|\cos\theta_i|}\int_{j\neq i} p(\hat{\mathbf{n}}_j, \hat{\mathbf{n}}_i)\, d\omega_j + \frac{1}{4\pi}\int_{j\neq i}\frac{f_{d\pm}^{j}}{|\cos\theta_j|} p(\hat{\mathbf{n}}_i, \hat{\mathbf{n}}_j)\, d\omega_j + S1_i f_{c-} + S2_i f_{c+} \qquad \text{(Eq. 5)}$$

The scattering coefficients $S1_i$ and $S2_i$ are related to the coefficients S_1 and S_2 in Eq.s (2) and (3). The explicit expressions for K, $S1_i$ and $S2_i$ will be discussed in Section 2.3.

For brevity, at this point we introduce following notations; μ_i is used for $\cos\theta_i$, and p_{ij} for $p(\hat{\mathbf{n}}_i, \hat{\mathbf{n}}_j)$. The explicit expr essions for p_{ij} will again be defer red to section 2.3. The integrals in Eq.s (4) and (5) can be evaluated using numerical integration techniques. Gaussian Quadrature is one of the well known numerical methods used for this purpose [8]. The method is preferred in this context since it gives exact answer when Legendre polynomials ar e integrated. In general p_{ij}s can be expanded in terms of Legendre polynomials. Using our abbreviated notations and replacing the integral by a summation, Eq.s (4) and (5) ar e combined to obtain the following equation:

$$\pm\frac{df_{d\pm}^{i}}{dx} = -\frac{Kf_{d\pm}^{i}}{|\mu_i|} - \frac{1}{4\pi}\frac{f_{d\pm}^{i}}{|\mu_i|}\sum_{\substack{j=1\\ j\neq i}}^{N-1} p_{ji}\delta\omega_j + \frac{1}{4\pi}\sum_{j}\frac{w_j f_{d\pm}^{j}}{|\mu_j|} p_{ij}\delta\omega_j + S1_i f_{c\pm} + S2_i f_{c\mp} \qquad \text{(Eq. 6)}$$

In Eq. (6), w_js are the weights obtained from the standard tables [8], suitable for the sampling points

employed to evaluate the integral. The finite solid angle $\delta\omega_j$ associated with jth propagation channel is defined as

$$\delta\omega_j = 2\pi \sin\theta_j \delta\theta_j \qquad \text{(Eq. 7)}$$

Equations (2), (3) and (6) can be written in a compact form using matrix notations as follows:

$$\frac{dF}{dx} = \mathbf{M}F \qquad \text{(Eq. 8)}$$

where F is the column vector given in Eq. (1) and $\mathbf{M}$ is the coefficient matrix. Explicit expressions for the elements of $\mathbf{M}$ can be obtained by expanding Eq.s (2, 3) and (6).

2. Solution method

Equation (8) represents a linear set of differential equations, general solution of which is given by

$$F_i = \sum_{j=0}^{N} A_{ij} c_j e^{\lambda_j x}, \quad i = 0, 1, \ldots\ldots, N \qquad \text{(Eq. 9)}$$

where λ_j's are the eigenvalues and A_{ij}s are the elements of the eigenvector corresponding to the coefficient matrix $\mathbf{M}$. c_js are constants computed using the boundary conditions, i.e., the reflectivity values at the two interfaces of the slab.

In general, two boundary conditions are obtained at two interfaces of the slab for each pair (forward and backward moving) of collimated and diffuse fluxes. Boundary conditions for each channel are constructed by equating the total forward-moving flux in that channel to the total backward-moving flux in the same channel. We assume that the light from the source enters the random medium of the slab through the first interface ($x = 0$) and leaves through the last interface ($x = d$). If the total input flux (collimated + diffuse) is 1, Φ_c is the collimated fraction of total input flux, then $(1 - \Phi_c)$ is the diffuse portion of the input flux. R_c is the Fresnel reflectivity of any of the slab interfaces. R_s is the reflectivity of the back plane for the collimated flux. For the collimated flux pair, we can write following two boundary conditions, at the first and the second interfaces respectively of the slab

$$f_{c+}(0) = \Phi_c(1 - R_c) + R_c f_{c-}(0) \qquad \text{(Eq. 10)}$$

$$f_{c-}(d) = R_s f_{c+}(d) \qquad \text{(Eq. 11)}$$

The boundary conditions for the diffuse fluxes are given by

$$f^i_{d+}(0) = D_i + r_i f^{N-1-i}_{d-}(0), \quad i = 1, \ldots, N/2-1 \qquad \text{(Eq. 12)}$$

$$f^i_{d-}(d) = \sum_{l=1}^{N/2-1} R_{il} f^l_{d+}(d), \quad i = N/2, \ldots, N-1 \qquad \text{(Eq. 13)}$$

In Eq. (12), D_i is the diffuse flux input in the ith channel inside the slab, r_i is the reflectivity at the first surface for the diffuse flux propagating in the ith channel. R_{il} is the fraction of forward moving diffuse flux in lth channel that is reflected at the last interface and enters the ith channel.

d in Eq.s (11) and (13) is called the optical thickness and is given by

$$d = (mC_{ext})t \qquad \text{(Eq. 14)}$$

where m is the number of scattering centres per unit volume of the random medium, C_{ext} is the extinction cross-section and t is the physical thickness of the slab.

3. Computation of k, S_1, S_2, K, $S1_i$, $S2_i$, and $p(\hat{\mathbf{n}}_i, \hat{\mathbf{n}}_j)$

Albedo, a_0 of a single particle is defined as the ratio of the scattering efficiency (Q_{scat}) and the extinction efficiency (Q_{ext}) and is given by[3]

$$a_0 = \frac{Q_{scat}}{Q_{ext}} \qquad \text{(Eq. 15)}$$

In case of spherical particles, a_0 is computed using Mie analytical theory[4].

k in Eq.s (2) and (3) can be shown to be the ratio of the extinction efficiency (Q_{ext}) and the absorption efficiency (Q_{abs}) of a single scattering centre[3]. k is given by

$$k = \frac{Q_{abs}}{Q_{scat}} \qquad \text{(Eq. 16)}$$

The difference between extinction efficiency and extinction cross-section is that the former is a number and thereby dimensionless while the later has the dimension of area. Following relation holds between C_{ext} and Q_{ext}:

$$C_{ext} = Q_{ext} \frac{\lambda^2}{4\pi} \qquad \text{(Eq. 17)}$$

The sum of S_1 and S_2 in Eq.s (2) and (3) is equal to a_0[3]. S_1 is given by

$$S_1 = 0.5\left(a_0 + \sum_{l=1,l\,odd}^{L} a_l W_l^2\right) \quad \text{(Eq. 18)}$$

S_2 is given by

$$S_2 = a_0 - S_1 \quad \text{(Eq. 19)}$$

S_1 and S_2 estimate the amount of light that is scatter ed from the collimated channel to the diffuse channels. W_ls are given by[4)]

$$W_l = \frac{1}{2} \quad for \quad l = 1$$
$$= \frac{(-1)(-3)\ldots\ldots(-l+2)}{(l+1)(l-1)\ldots\ldots 2} \quad for \quad l \geq 3 \quad \text{(Eq. 20)}$$

The coefficients a_ls are obtained a normalization of the phase function, as explained below.

We use $K = 2k$, when the specific intensities ar e completely diffuse and almost isotropic. $p(\hat{\mathbf{n}}_i, \hat{\mathbf{n}}_j)$ (or, p_{ij} in compact notation) is a function of cosγ, γ being the angle between $\hat{\mathbf{n}}_i$ and $\hat{\mathbf{n}}_j$. Expressing the phase function as a sum of Legendr e polynomials we can write the following

$$p(\hat{\mathbf{n}}_i, \hat{\mathbf{n}}_j) = \sum_l a_l P_l(\cos\gamma) \quad \text{(Eq. 21)}$$

where the symbol P_l stands for Legendre polynomial of order l, and a_l is the lth coefficient. cosγ is given by

$$\cos\gamma = \hat{\mathbf{n}}_i \cdot \hat{\mathbf{n}}_j = \cos\theta_i \cos\theta_j + \sin\theta_i \sin\theta_j \cos(\phi_i - \phi_j) \quad \text{(Eq. 22)}$$

Since our propagation channels are not ϕ dependent, a phase function obtained by integrating Eq. (22) w.r.t ϕ_i, ϕ_j would be sufficient for our purposes[4)]. Hence, integrating Eq. (22), we obtain

$$p(\hat{\mathbf{n}}_i, \hat{\mathbf{n}}_j) = P_{ij} = \sum_l^L a_l P_l(\cos\theta_i) P_l(\cos\theta_j) \quad \text{(Eq. 23)}$$

The values of a_l and the total number of Legendr e polynomial terms, L depend on the scattering characteristics of individual scattering centr es. Scattering due to transpar ent, spherical par ticles of size larger t han t he o perating wa velength i s m ostly anisotropic in nature, i.e., light is mostly scattered in the forward direction. Hence in this particular case, L is taken to be half the total number of diffuse channels[10)]. In case of isotropic scattering, L may not be that large.

a_ls are obtained from following normalization integral,

$$a_l = \frac{(l+0.5)}{a_0} \int_{-1}^{1} p_0(\theta) P_l(\cos\theta) d(\cos\theta) \quad \text{(Eq. 24)}$$

All a_ls are normalized by a_0. In Eq. (24), $p_0(\theta)$ is computed using the angle dependent scatter ed intensity as follows,

$$p_0(\theta) = |E_s|^2 \sin\theta \quad \text{(Eq. 25)}$$

where E_s is the θ-dependant part of the scatter ed electric field at a point far ($kr >> \lambda$) from a scattering centre.

$S1_i$ and $S2_i$ are computed as follows

$$S1_i = \frac{1}{4\pi} p(\cos\theta_i, 1)\delta\omega_i \quad \text{(Eq. 26)}$$

$$S2_i = \frac{1}{4\pi} p(\cos\theta_i, -1)\delta\omega_i \quad \text{(Eq. 27)}$$

Eq.s (26), and (27) show that $S1_i$ and $S2_i$ are the fraction of scattered light entering the ith channel from 0th and Nth channels respectively.

For spherical inclusions, Mie analytical theory can be used to compute C_{scat}, C_{ext} and E_s as a function of operating wavelength, radius and refractive index of inclusions. In case of non-spherical inclusions, a combination of FDTD with far-field method can be used to compute the above quantities numerically.

In all calculations presented here the widths of the propagation channels are unequal and are determined using Gaussian quadrature sampling points. The viewing directions outside the slab are computed using the Snell's law from inner propagation channels. Mathcad application software is used to write the SRTE code.

Recursive Convolution Finite-Difference Time-Domain Method

1. Near-field generation

The 3D Finite-dif ference time-domain (FDTD) method is used to compute the scattering characteristics of a non-spherical inclusion. The program implements the 1st order Drude model permittivity for noble metals using a recursive convolution framework. The 3D program is an extension of our 2D algorithm implementing Maxwell's equations.

Maxwell's equations for materials with fr equency dependent dielectric constant are given by

$$\mu_M \partial_t \mathbf{H}(\mathbf{r}, t) = -\nabla \times \mathbf{E}(\mathbf{r}, t) \quad \text{(Eq. 28)}$$

$$\partial_t \mathbf{D}(\mathbf{r}, t) = \nabla \times \mathbf{H}(\mathbf{r}, t) \quad \text{(Eq. 29)}$$

where μ_M is the magnetic permeability, taken to be constant and equal to vacuum permeability, $\mathbf{H}$ is the magnetic vector, $\nabla \equiv \hat{\mathbf{x}}\frac{\partial}{\partial x} + \hat{\mathbf{y}}\frac{\partial}{\partial y} + \hat{\mathbf{z}}\frac{\partial}{\partial z}$ is the vector differential operator, $\times$ stands for vector curl operation. In this notation ∂_t denotes $\partial/\partial t$. $\mathbf{D}$ is the displacement current, given by

$$\mathbf{D}(\mathbf{r}, \omega) = \varepsilon(\mathbf{r}, \omega)\mathbf{E}(\mathbf{r}, \omega) \quad \text{(Eq. 30)}$$

where $\mathbf{E}$ is the electric vector and ε is the dielectric constant. The time domain behavior of $\mathbf{D}$ is obtained by taking the inverse Fourier transform on both sides of Eq. (30), and using the convolution theorem. We find[6)]

$$\mathbf{D}(t) = \int_0^t \varepsilon(\tau)\mathbf{E}(t-\tau)d\tau \quad \text{(Eq. 31)}$$

where $\varepsilon(t) = \mathrm{F}^{-1}\{\varepsilon(\omega)\}$, and F^{-1} denotes the inverse Fourier transform operator.

In the first-order Drude model, $\varepsilon(\omega)$ is given by

$$\varepsilon(\omega) = 1 + \frac{\omega_p^2}{\omega(i\nu_c - \omega)} = \varepsilon_\infty + \chi(\omega) \quad \text{(Eq. 32)}$$

where ω_p is the plasma frequency, ν_c is the collision frequency, ε_∞ is infinite frequency dielectric constant and equal to 1 and $\chi(\omega)$ is the susceptibility. Taking the inverse Fourier transform of $\chi(\omega)$ we find[6)],

$$\chi(t) = \frac{\omega_p^2}{\nu_c}\left[1 - e^{-\nu_c t}\right] U(t) \quad \text{(Eq. 33)}$$

where $U(t)$ is a unit step function defined by

$$\begin{aligned} U(t) &= 0 \quad if \quad t = 0, \\ &= 1 \quad t > 0 \end{aligned} \quad \text{(Eq. 34)}$$

In order to evaluate Eq. (31), we first r eplace $\varepsilon(\tau)$ by the inverse Fourier transform of $\varepsilon(\omega)$. The resulting form is discretized in keeping with FDTD time stepping scheme. If Δt is the minimum time step, and if n represents the total number of time steps corresponding to time instant t, then $t = n\Delta t$. Taking field $\mathbf{E}$ to be constant over any single interval $[m\Delta t, (m+1)\Delta t]$, where $m \in 0, \ldots, n$, the integral in Eq. (31) reduces to a partial summation as follows: [6)]

$$\mathbf{D}^n = \varepsilon_0\varepsilon_\infty\mathbf{E}^n + \varepsilon_0\sum_{m=0}^{n-1}\mathbf{E}^{n-m}\int_{m\Delta t}^{(m+1)\Delta t}\chi(\tau)d\tau \quad \text{(Eq. 35)}$$

Equation (35) can be written in the following compact form

$$\mathbf{D}^n = \varepsilon_0\varepsilon_\infty\mathbf{E}^n + \varepsilon_0\Psi^n \quad \text{(Eq. 36)}$$

where,

$$\begin{aligned} \Psi^n &= \sum_{m=0}^{n-1}\mathbf{E}^{n-m}\int_{m\Delta t}^{(m+1)\Delta t}\chi(\tau)d\tau \\ &= \sum_{m=0}^{n-1}\mathbf{E}^{n-m}\frac{\omega_p^2}{\nu_c}\left[\Delta t + \frac{e^{-\nu_c(m+1)\Delta t} - e^{-\nu_c(m)\Delta t}}{\nu_c}\right] \end{aligned} \quad \text{(Eq. 37)}$$

The vector quantity, Ψ, is known as the accumulation field.

The update equation for the magnetic field is given by

$$\mathbf{H}^{n+1/2} = \mathbf{H}^{n-1/2} - \frac{\Delta t}{\mu_M h}\mathbf{d} \times \mathbf{E}^n \quad \text{(Eq. 38)}$$

The superscripts n, $n+1/2$ or $n-1/2$ represent the time steps at which corresponding quantities are evaluated. $\mathbf{d}$ is the 2nd order accurate, central, finite-dif ference approximation of the vector dif ferential operator (∇). $\mathbf{d}$ is of the form ($\mathbf{d} \equiv \hat{\mathbf{x}}d_x + \hat{\mathbf{y}}d_y + \hat{\mathbf{z}}d_z$), where $d_x f(x, y, z)$ is given by

$$d_x f(x,y,z) = f(x + h/2, y, z) - f(x - h/2, y, z) \quad \text{(Eq. 39)}$$

Following Eq. (39), similar expressions can be written for $d_y f(x, y, z)$ and $d_z f(x, y, z)$. Δt and h are the time and space steps respectively.

In the non-dispersive case of FDTD, the update equation for the magnetic field will be the same as Eq. (38).

The update equation for the electric field is given by

$$\mathbf{E}^{n+1} = \mathbf{E}^n - \frac{1}{\varepsilon_\infty}(\Psi^{n+1} - \Psi^n) + \frac{\Delta t}{\varepsilon_0\varepsilon_\infty h}\mathbf{d} \times \mathbf{H}^{n+1/2} \quad \text{(Eq. 40)}$$

The superscripts $n+1$, n, and $n+1/2$ indicate the time steps at which corresponding quantities are evaluated. ε_∞ is the infinite frequency dielectric constant and is taken to be 1. ε_0 is the dielectric constant of vacuum and is taken to be 1.

$\Psi^{n+1} - \Psi^n$ in Eq. (40) is computed using a r ecursive equation obtained using Eq. (37) and is given by

$$\Psi^{n+1} - \Psi^n = c_1\mathbf{E}^n + c_2\left[\Psi^n - \Psi^{n-1}\right] \quad \text{(Eq. 41)}$$

Ψ at zero-th and all negative time steps are identically zero. Ψ at any positive time step can be obtained using Eq. (41). Physically Ψ represents a convolution of electric field and dielectric constant of metal. c_1 and c_2 in Eq. (41) are given by

$$c_1 = \frac{\omega_p^2}{v_c}(1 - e^{-v_c}), \quad c_2 = e^{-v_c} \qquad \text{(Eq. 42)}$$

The update equation for the electric field in case of non-dispersive FDTD is given by

$$\mathbf{E}^{n+1} = \mathbf{E}^n + \frac{\Delta t}{\varepsilon_0 h}\mathbf{d} \times \mathbf{H}^{n+1/2} \qquad \text{(Eq. 43)}$$

We computed c_1 and c_2 at each wavelength using measured value of complex metal dielectric constant. If $\varepsilon(\omega)$ is the dielectric constant of metal at a frequency ω, then we can write

$$\varepsilon(\omega) = \varepsilon_1(\omega) + i\varepsilon_2(\omega) \qquad \text{(Eq. 44)}$$

where $\varepsilon_1(\omega)$ and $\varepsilon_2(\omega)$ are the real and imaginary parts respectively. c_1 and c_2 can be expressed in terms of $\varepsilon_1(\omega)$ and $\varepsilon_2(\omega)$ as follows

$$c_2 = e^{\frac{\varepsilon_2 \omega}{1-\varepsilon_1}} \qquad \text{(Eq. 45)}$$

$$c_1 = -\frac{\omega}{\varepsilon_2}\left((1-\varepsilon_1)^2 + \varepsilon_2^2\right)[1 - c_2] \qquad \text{(Eq. 46)}$$

This RC-FDTD algorithm is developed for monochromatic applications and the incident field is generated with a pair of current sources. The scattered field at each grid point is computed as follows:

$$\mathbf{E}_s = \mathbf{E}_t - \mathbf{E}_i \qquad \text{(Eq. 47)}$$

where $\mathbf{E}_s$, $\mathbf{E}_t$, and $\mathbf{E}_i$ are the scattered, total and incident electric field vectors respectively.

2. Near-to-far field transformation

RC-FDTD can only be used to generate the near field values. Hence, we used a Rayleigh-Sommerfield integral to generate the far-field from the near field values obtained using FDTD. $E(R)$, an electric field component (scalar) computed at a far-field point by numerically integrating the near field values E, generated by FDTD on the surface of a rectangular parallelepiped S (surface area = Σ) enclosing the scatterer[11]. R is the radial distance of the far-field point from any point on the surface of integration. If $\hat{n}$ is the unit normal drawn outward at each point on S, the near-to-far field transformation integral is given by

$$E(R) = \frac{1}{\Sigma}\int_S \left\{\frac{e^{ikR}}{R}\nabla E - E\nabla\left(\frac{e^{ikR}}{R}\right)\right\} \cdot \hat{n}\, dS \qquad \text{(Eq. 48)}$$

The integral in Eq (45) is numerically evaluated by taking 180 samples in polar angle θ and 36 samples in the azimuth angle ϕ.

Simulation method

The simulation method consists of following steps:

1) Monte Carlo method
2) Numerical computation of extinction and scattering cross-sections and the phase function

Details of computation steps are described in following subsections.

1. Monte-Carlo method

We generate a cluster by impregnating a sphere made of the binder medium, with randomly distributed metal particles. A random number generator generates random particle configurations. The random number generator is a computer code that outputs pseudo-random numbers drawn from a uniform distribution[12]. In this work the random number generator is used to generate a random spatial distribution of inclusions. To change the configuration, each time, the random number generator is called with a new seed. The seed is set to be equal to the current time obtained from the computer clock.

2. Numerical computation of extinction and scattering cross-sections and the phase function

A 3D FDTD algorithm implementing 1st order Drude model is employed to compute the extinction, scattering cross-sections and the phase function due to this cluster of metal particles. The extinction efficiency is computed as follows[11]

$$Q_{ext} = -\frac{(4\pi)v}{8\pi Ii}\left\langle \mathrm{Re}\,(\mathbf{E}_i \cdot \mathbf{E}_s^*)_{\theta=0^\circ}\right\rangle \qquad \text{(Eq. 49)}$$

where $\mathbf{E}_i$ and $\mathbf{E}_s^*$ are the incident field vector and the complex conjugate of the scattered field vector respectively, computed at a far-field point of the cluster in the forward scattering direction ($\theta = 0^\circ$, θ being the polar angle). Angular brackets denote an average over one time period. v and Ii are the speed of light and incident intensity respectively. The scattering efficiency is given by

$$Q_s = \frac{v}{8\pi Ii}\int_{\phi=0}^{2\pi}\int_{\theta=0}^{\pi}\left\langle |E_s|^2 \right\rangle \sin\theta\, d\theta\, d\phi \qquad \text{(Eq. 50)}$$

The far fields in Eq.s (49) and (50) are computed using FDTD and Eq. (48). The phase function is computed using Eq. (25), where the scattered electric field E_s is computed in the far-field as a function of the polar angle θ.

The cross-sections and the phase function are computed for m different random distributions of the par ticles in the cluster. Finally, these quantities, averaged over all m distributions, are used to compute the scattering and absorption coef ficients (Section 2.3) used in the SR TE for mulations. This is done to simulate a medium where an average cluster serves as a single scattering centre.

Results and discussion

It turns out that the SRTE formulation outlined in this paper is suitable for diffuse illumination. For coherent illumination, such as that due to laser , the parameter K used in Eq. (6) has to be changed. K is also related to the absorption coefficient of the material of the par ticles. These facts become evident fr om **Fig. 1**, where, we compute the angular spectrum of diffuse transmittance of a dielectric slab impr egnated with spherical inclusions of non-absorbing material. Results are computed using a 42-channel SRTE, where the 40 diffuse channels are defined by the Gaussian quadrature points for the polar angle θ. The 0^{th} and 41^{st} channels ar e r eserved for collimated transmission and reflection respectively. The number of Legendre polynomial ter ms in the expansion of the phase function is taken to be 20. The number of Bessel function and Legendre polynomial terms in the expansion of Mie analysis is determined as a function of the inclusion radius[4]. In this case, the phase function and the extinction, scattering cross-sections of individual scattering centres are computed analytically using the Mie theory[5]. The computed angular spectr um is compar ed with the data obtained experimentally.

In case of experiment following specifications ar e chosen: the refractive index of the dielectric material of the slab is n_m = 1.53. The slab material is impr egnated with dielectric spherical inclusions of refractive index n_s = 1.59. The transmittance is recorded at 2° interval of the viewing angle outside the slab. Laser beam at 540nm wavelength is used as the incident light. Volume fraction of inclusions is 0.259. The inclusion radius is 1.5μm. The slab width is 12μm.

In the first set of computed data (Computation 1), $K = 2k$, as mentioned in Section 2.3. In the second set of computed data (Computation 2), $K = 2Q_{abs}$. For both sets of computed data, n_m = 1.52, n_s = 1.59 + i0.001 and the incident illumination is taken to be completely coherent. **Fig. 1** shows that the 1^{st} set of computed data are widely different from the measured data. The second set of r esults can approximately predict the experimental findings. The transmittance is shown as a function of viewing angles (polar angle θ, corresponding to dif ferent channels) outside the slab. The transmittances in **Fig. 1** are plotted in log scale.

The discrepancies between the computed and measured data might be traced to the inappropriateness of the phase function. Since experimental set-up uses a laser as the sour ce of illumination, the experimental phase function and scattering extinction cr oss-sections are dif ferent fr om Mie analytical r esults which ar e obtained for infinite, plane wave incidence. Fur thermore, it should be noted that Mie analytical for mulae are convergent for small par ticles, the same for mulae result in divergent and non-stable values as the particle radius increases. In addition, some discr epancies are found in the measured data, hence there is a need for more accurate and reliable measurement data.

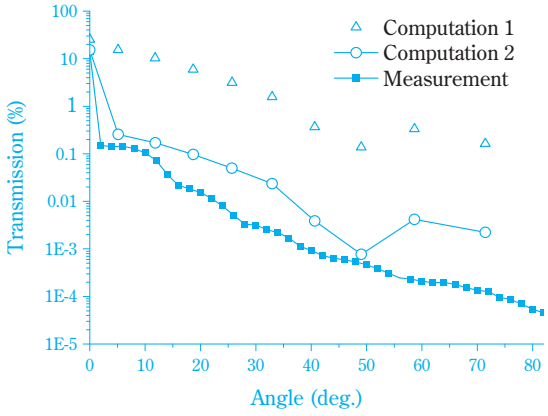

Fig. 1 shows the comparison between the computed and measured angular spectra of diffuse transmittance of a slab, containing monodisperse spherical inclusions of radius 1.5μm as a function of viewing angles.

To demonstrate the usefulness of the computation scheme developed here, we compute the transmittance spectrum of a slab containing non-spherical scattering

centres resulting from cluster formation. In case of cluster formation in the medium, we compute the scattering characteristics (phase function and scattering, extinction cross-sections) numerically using a combination of FDTD and a near-to-far field transformation integral (Section 3) of a computationally generated cluster consisting of randomly distributed inclusions. The incident light is polarized along the x-axis and pr opagating along the z-axis. The plane wave incident beam is simulated by introducing periodic boundary conditions over the bounding faces of the computational domain those are not nor mal to z-axis (bounding sur faces other than those parallel to xy-plane). The computational domain is terminated using absorbing boundary conditions along the z-direction. The scattering characteristics are averaged over 50 different random configurations of clusters. In the example pr esented here we consider a nanocluster of metallic inclusions.

Fig. 2 shows the cross-sections of a typical computer-generated cluster in three orthogonal planes. The refractive index of the sur rounding medium and the host matrix is 1.5. The volume density of inclusions is 50%. Radius of each inclusion is 10nm.

Fig. 3 shows the diffuse reflectance spectra of a slab illuminated using completely diffuse light. For each wavelength, diffuse flux propagation is computed in 40 channels. Data presented in **Fig. 3**, are summed over all the 40 propagation channels for each wavelength. The slab is made of r esin (refractive index = 1.5), impr egnated with silver par ticles [wavelength dependent complex refractive indices are obtained from Ref. 13]. Volume density of the silver particles is 5%. In case of FDTD (solid line), each particle is a cluster made up of individual spherical inclusions (radius 10nm). The volume density of the inclusions in the cluster is 50%. The radius of the cluster is 100nm. By cluster radius we mean the radius of the spherical volume that contains all the metal inclusions in one cluster.

Slab thickness is 1μm. In case of Mie computation (dotted line) each par ticle is a spher e with radius 100nm of effective refractive index and Mie theory is used to compute the cr oss-sections and the phase function. The effective refractive index of the sphere is computed using Maxwell Garnet theory (MGT) assuming all perfectly spherical inclusions[11].

Fig. 3 indicates that FDTD computation yields a smoother variation of transmission compared to that obtained using MGT. We plan to measure the transmission spectra of films of metal paint to validate the accuracy and applicability of our approach.

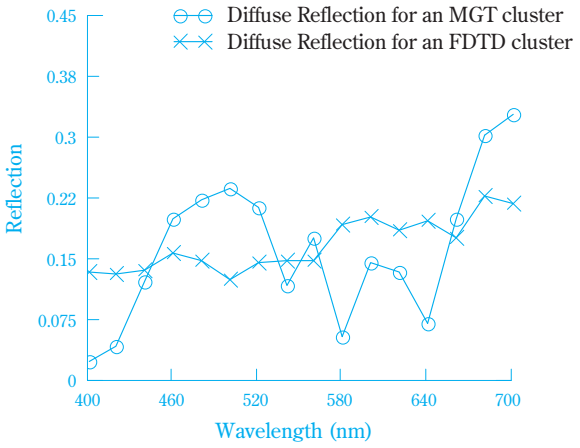

Fig. 3 Diffuse reflectance spectra of a slab of a composite medium computed using the SRTE; 1) individual scattering centre is a sphere of effective refractive index computed using MGT and the corresponding scattering characteristics are computed using Mie theory, 2) individual scattering centre is a cluster, corresponding scattering characteristics are computed using the FDTD and the near-to-far field transformation integral.

Fig. 2 The cross-sections of a cluster in three orthogonal planes;
a) xy-plane, b) yz-plane, c) zx-plane. Black dots show the positions of inclusions.

Conclusions

In this paper we implement an N-flux SR TE to compute the collimated and diffuse reflection and transmission spectra of a slab of random medium. The medium of the slab is formed by impregnating a homogeneous medium with random distribution of inclusions with refractive index different from the host medium. In case of spherical inclusions the scattering characteristics (scattering, extinction cross sections and phase function) used in SRTE formulations are computed using Mie analytical theory. In case of non-spherical inclusions, we propose a numerical method incorporating FDTD and a near-to-far field transformation to compute the average scattering characteristics of a single scattering centre. Finally, the numerically computed average scattering characteristics of a single scattering centre are used in the SR TE formulation to obtain the collimated or the angle-dependent diffuse transmittance. We demonstrate the application of our computation method for a slab consisting of metal nanoclusters that serve as non-spherical scattering centres. Although, the results presented here concern metal clusters only, the same approach can also be adopted in case of non-metallic clusters and metallic or non-metallic single particle inclusions of arbitrary shape.

References

1) Murata, "Industrial Colorimetry," Sumitomo Chemical Corporation, 1968 (in Japanese).
2) Chandrasekhar, S., *Radiative Transfer*, Dover Publications Inc., New York, 1960.
3) P. S. Mudgett, and L.W. Richards, "Multiple scattering calculations for technology", Applied Optics, vol.10, no.7, 1971.
4) A. Ishimaru, Wave propagation and scattering in random media, IEEE Press, New York, 1997.
5) Barber, P.W., and Hill, S.C., *Light scattering by particles: computational methods, World Scientific*, Singapore, 1990.
6) K. S. Kunz, and R. J. Luebbers, *The Finite difference Time Domain Method for Electromagnetics*, Chapter 8, CRC Press, Boca Raton, pp.123-162, 1993.
7) S. Banerjee, T. Hoshino, and J. B. Cole, "Subwavelength Metallic Grating Simulation using an implementation of recursive convolution FDTD", JOSA A, **25** (8), 1921-1928 (2008).
8) B.E Burrows, Chi O. AO, F.L. Teixeira, J.A. Kong, L. Tsang, "Monte Carlo simulation of Electromagnetic wave propagation in dense random media with dielectric spheroids", IEICE Trans. Electron. Vol.E83-C, no.12, Dec. 2000, pp. 1797.
9) M. Abramowitz, and I. A. Stegun, eds. (1972), "Section 25.4, Integration", *Handbook of Mathematical Functions (with Formulas, Graphs, and Mathematical Tables)*, Dover.
10) A. da Silva, M. Elias, C. Andraud and J. Lafait, "Comparison of the auxiliary function method and the discrete-ordinate method for solving the radiative transfer equation for light scattering", J. Opt. Soc. Am. A, vol.20, no.12, 2003.
11) C.F Bohren, and D. R. Huffman, Absorption and scattering of light by small particles, (Wiley-VCH Verlag GmbH & Co. kGaA, Weinheim, 2004).
12) Press, W. H., Flannery, B. P., Teukolsky, S. A. & Vetterling, W. T. (1992), *Numerical recipes in C. The Art of Scientific Computing*, second ed., Cambridge University Press.
13) P.B. Johnson and R. W. Christy, "Optical constants of the noble metals", *Phys. Rev. B*, vol.6, no.12, p.4370, 1972.

PROFILE

Saswatee Banerjee

Sumitomo Chemical Co., Ltd.
IT-Related Chemicals Research Laboratory
Research Associate

Kiyoharu Nakatsuka

Sumitomo Chemical Co., Ltd.
IT-Related Chemicals Research Laboratory
Senior Research Specialist